Biophys. Struct. Mechanism 2, 43—59 (1976)

Biophysics of Structure and Mechanism

Subunit Symmetry of Tetrameric Phosphorylase *a*

K. Bartels* and P. M. Colman**

Max-Planck-Institut für Biochemie and Physikalisch-Chemisches Institut der Technischen Universität, D-8033 Martinsried, Fed. Rep. Germany

Abstract. Native crystallographic data of tetrameric phosphorylase *a* crystals, space group $P2_1$, have been collected photographically to 3 Å resolution. These data have been used in Patterson search methods in reciprocal and real space.

The tetramers were found to exhibit molecular 222 symmetry. The cross vector between the centres of the two symmetry related tetramers in the unit cell was determined by two different translation function methods.

On the basis of these rotation and translation function results a model for the arrangement of monomers within the tetramer and of tetramers in the unit cell is proposed.

The 222 symmetry of the tetrameric molecule is found only when high resolution diffraction data are included (*i.e.* higher than 6 Å). At lower resolution other symmetries dominate.

Calculations with the proposed model have shown that these spurious symmetries result from the nonspecific overlap of protein-protein and solvent-solvent cross vectors.

These results emphasize the importance of high resolution data when non-crystallographic symmetry of globular proteins is studied.

Key words: Glycogen Phosphorylase — Subunit Symmetry — Non-crystallographic Symmetry — Rotation Function — Translation Function.

Introduction

Phosphorylase (E.C.2.4.1.1.) is the key enzyme for the breakdown of glycogen. It exists in two interconvertible forms. The *b* form, which under physiological conditions is a dimer, is inactive without effectors, such as AMP, IMP and/or Glucose-1-P. Phosphorylase kinase converts phosphorylase *b* into the *a* form which

* Extract from Dissertation, Technische Universität München.

** Present address: Dept. of Inorganic Chemistry, University of Sydney, Australia.

in solutions at concentrations around 0.2 to 10 mg exists as a tetramer and is active without effectors, but its activity is enhanced by AMP.

In 1972 we reported crystallization of both glycogen phosphorylase *a* and *b*. Both enzymes derived from rabbit muscle were crystallized in a tetrameric form (MW = 400000) in the presence of AMP. The two crystal forms were isomorphous in space group $P2_1$, with a = 119.4 Å, b = 188.6 Å, c = 88.2 Å, $\beta = 108.6°$; $V = 1.88 \cdot 10^6$ Å^3 (Fasold *et al.*, 1972). Apparently identical crystals have been reported by F. S. Mathews (1967) and Madsen *et al.* (1972). Four chemically identical subunits of MW 100000 are contained in the asymmetric unit.

From electron micrographs it was concluded that these four subunits are arranged on the vertices of a tetrahedron according to point symmetry 222 (Kiselev *et al.*, 1971; 1974). These optically filtered micrographs show resolved monomers of elongated bent shape. Johnson *et al.* (1974) reported the crystal structure of dimeric phosphorylase *b* with IMP at 6 Å resolution, showing a rather compact molecule, but they have not yet been able to resolve the monomer-monomer-contact within the dimer.

Phosphorylase *b* with IMP and phosphorylase *b* and *a* with AMP have been shown by ESR measurements to be in different conformational states (Campbell *et al.*, 1972; Dwek *et al.*, 1972; Griffiths *et al.*, 1974). A structure analysis of the tetrameric form and its comparison with the dimer might show the structural differences responsible for the different functional properties. This communication describes crystallographic data collection and the analysis of the subunit symmetry which leads to a preliminary model of the crystal structure of tetrameric phosphorylase *a*.

Methods, Results and Discussion

I. Crystallographic Intensity Data Collection

Crystallographic data were collected by the screenless precession technique, using a focus to crystal and crystal to film distance of 300 mm and 100 mm respectively. The source was graphite monochromatized Cu K_α radiation from a sealed tube operated at 1.2 kW. The cameras were equipped with long collimators (200 mm). Pinholes of 0.3 to 0.5 mm were used depending on the crystal size.

Each crystal[1] tolerated about 250 hrs irradiation time, thus providing between 1 and 5 intensity data photographs, depending on the crystal size. A precession angle of 1.5° was used, yielding theoretically about 8500 reflexions (up to 3 Å resolution) per film.

24000 out of 73000 crystallographically independent reflexions out to 3 Å resolution (60000 observations) were measured significantly above background ($> 1.5\,\sigma$), using the film evaluation programs by Schwager and Bartels (1975); cf. Fig. 1.

Refinement of the crystal orientation parameters (Schwager *et al.*, 1975) proved to be critical: the R_{sym}-value for individual films cannot be used as a monitor of satisfactory evaluation because of the almost complete absence of symmetry-equivalent reflexions on the films. (The long crystal axis b, which is the crystallo-

[1] The crystals used in this work were kindly provided by H. Fasold and coworkers, Institut für Biochemie der Universität Frankfurt.

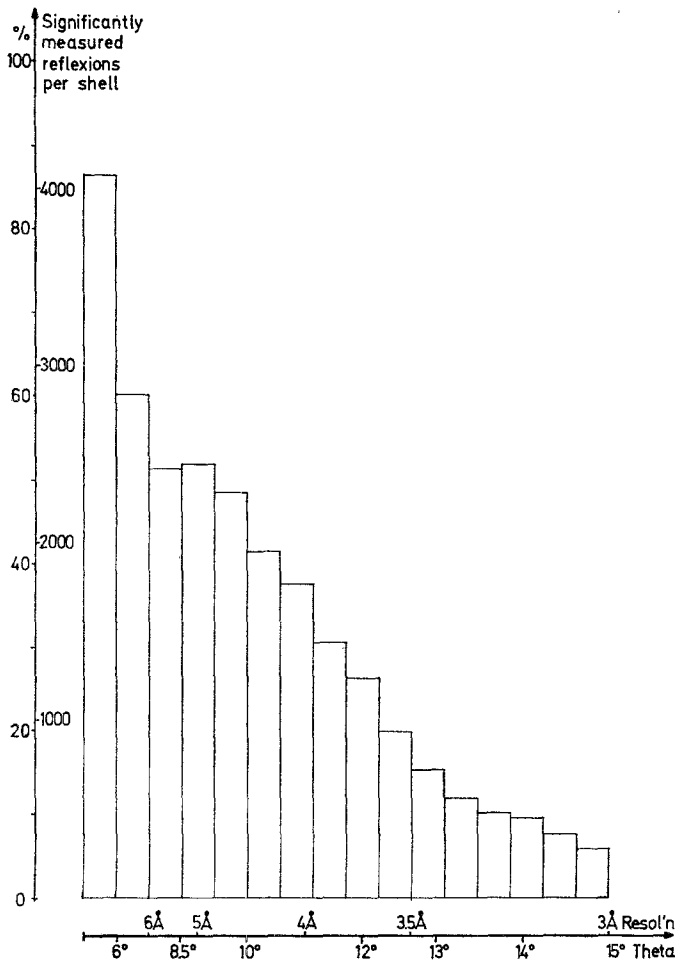

Fig. 1. Histogram of significantly measured reflexions within shells of equal reciprocal space volume

graphic twofold screw axis, lies in the direction of the smallest crystal dimension, so that it is difficult to mount this axis parallel to the spindle axis on the camera.) Absorption correction (Schwager *et al.*, 1973) was applied wherever the crystals were sufficiently large.

No twinning of the crystals was observed.

The data of 62 films were merged using individual scaling and temperature factors for each film (Steigemann, 1974). The final R-value for symmetry-equivalent intensities is $R_{\text{lin}} = 0.13$. The following definition of the R value is used:

$$R_{\text{lin.}} = \left(\sum_j \sum_{i=1}^{n_j} | I_{ij} - \bar{I}_j |\right) / \sum_j n_j \bar{I}_j,$$

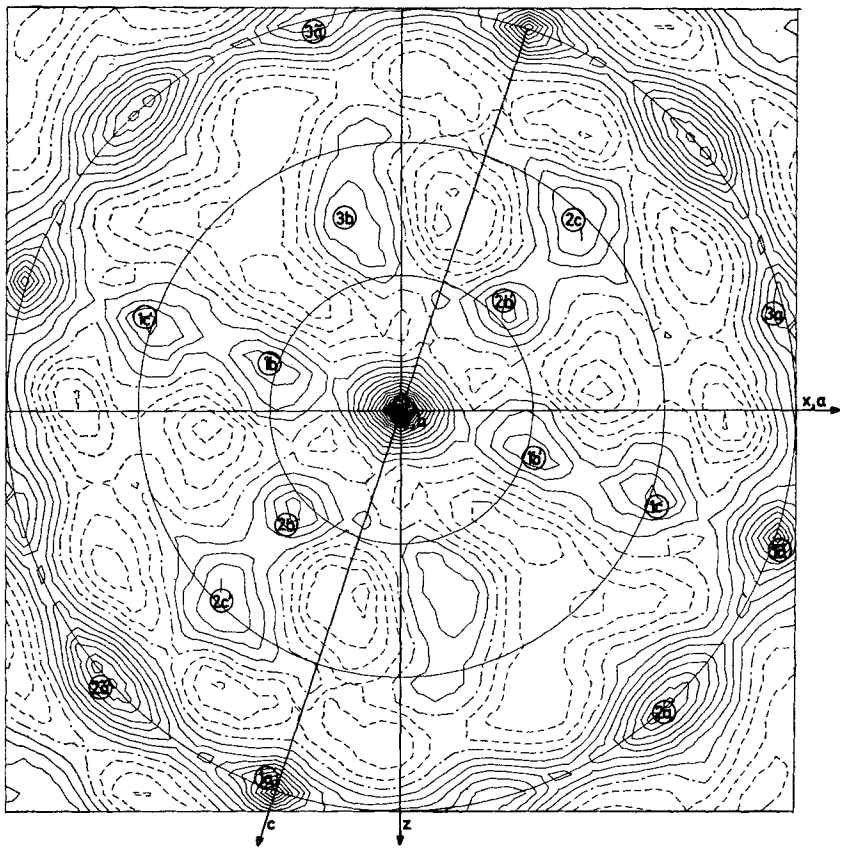

Fig. 2. Stereogram for twofold axes derived from real space rotation function, using the 3 Å-Patterson map calculated from all data available. Interpretation is given in the text. All stereograms shown in this paper use the polar angle definition given by Rossmann and Blow (1962). The radius is proportional to ψ whereas the polar angle is identical with φ. The circles indicate $\psi = 30°, 60°, 90°$

where j indicates independent reflexions, n_j is the number of individual measurements i for the jth reflexion and $\bar{I}_j$ the mean value $(\sum_{i=1}^{n_j} I_{ij})/n_j$. The sum over j includes only reflexions with $n_j \geq 2$.

II. Non-Crystallographic Symmetry

a) Rotation Function: Patterson self-rotation functions (Rossmann and Blow, 1962) were calculated for different resolution and radius ranges, using Crowther's fast rotation function program in reciprocal space (Crowther, 1972) and a real space Patterson search routine (Fehlhammer, 1975; Hoppe, 1957; Huber, 1970).

Regrettably the orthogonalization conventions of the two programs differ and consequently the derived stereograms are differently oriented. Crowther's program puts the monoclinic **b** and **c** axes parallel to **z** and **x**, respectively; the **y** axis is then

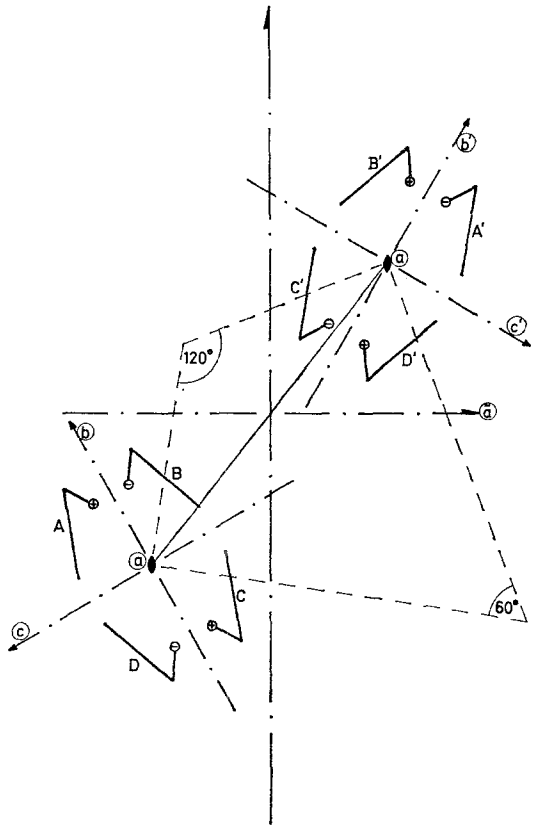

Fig. 3. Schematic model of the tetramers and their local symmetry axes within the $P2_1$ cell projected along the **c**-axis. The crystallographic **b** screw axis is drawn vertically. Its combination with the 3 different local rotation axes produces 3 local screw axes, only one of which is a proper rotation axis in the Patterson function [(ã), shown horizontally, parallel to the **a*** axis]; the other two are improper rotations (60°, 120°) the rotation angle being twice the inclination angle of the local diad axes to the crystallographic screw axis

parallel to **a***. Huber's **x** and **y** axes lie in the unit cell directions **a** and **b**, respectively, so **z** is parallel to **c***.

Fig. 2 is a stereogram for twofold axes ($\varkappa = 180°$)[2], derived from real space rotation, using the 3 Å-Patterson map calculated from all data available. The radius of integration around the Patterson function origin was 35 Å; the origin peak was excluded by using an inner radius limit of 6 Å. Essentially the same plot

[2] The polar angle convention used here is that given by Rossmann and Blow (1962). Note that the associated matrix given in their paper should be transposed (Tollin *et al.*, 1966). The rotation axis direction is defined by two polar angles ψ and φ, the rotation angle around this axis is $\varkappa$. ψ is the inclination of the rotation axis to the **y** axis (which in the monoclinic space group is unique); φ is in the **x**-**z**-plane and gives the angle between the **x**-axis and the projection of the rotation axis onto that plane in a mathematically positive rotation sense (the **z** axis has $\varphi = 270°$).

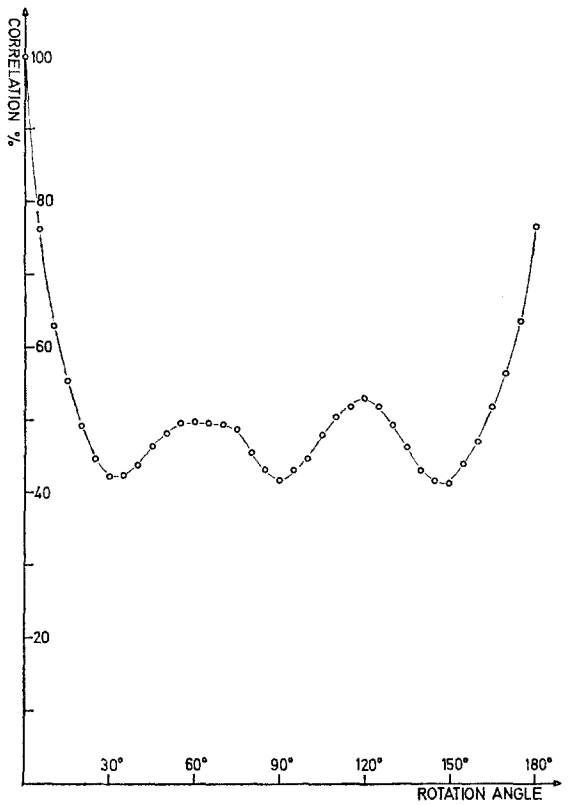

Fig. 4. Polar angle scan, $\psi \equiv 90°$, $\varphi \equiv 71.34°$; *i.e.* the rotation axis is kept constant and coincident with the c-axis. $\varkappa = 0°$ means identity of the two vector sets which yields 100% correlation. $\varkappa = 180°$ is the local twofold (1a). $\varkappa = 60°$ and 120° are improper rotations [giving rise to theoretically half the peak height of (1a)], which are the local screw axes indicated in Fig. 3

was obtained when using only a thin shell of the Patterson map between 10 Å and 15 Å radius.

Apart from the crystallographic screw axis the highest features in the stereogram are the peaks indicating twofold axes parallel and perpendicular to the c-axis, marked (1a) and (1ã), which in addition are perpendicular to the crystallographic 2-fold axis. (Molecular rotation axes are encircled in the figures and set in parantheses in the text; unit cell axes are not.) If these three directions were to indicate the molecular 222 symmetry, the Patterson function would have to show a pseudo origin peak of theoretically half the origin peak height on the Harker plane at $y = b/2$, as was found for example in asparaginase (Epp *et al.*, 1971) and aldolase (Eagles *et al.*, 1969). Nowhere in the Patterson map was such an outstanding feature found (cf. Fig. 10). Furthermore it will be demonstrated below that (1ã) contains a translation component.

However the peaks marked (1b) and (1c), or (1b′) and (1c′) resp., may be combined with (1a) to form two sets of mutuallay perpendicular diads, the two sets

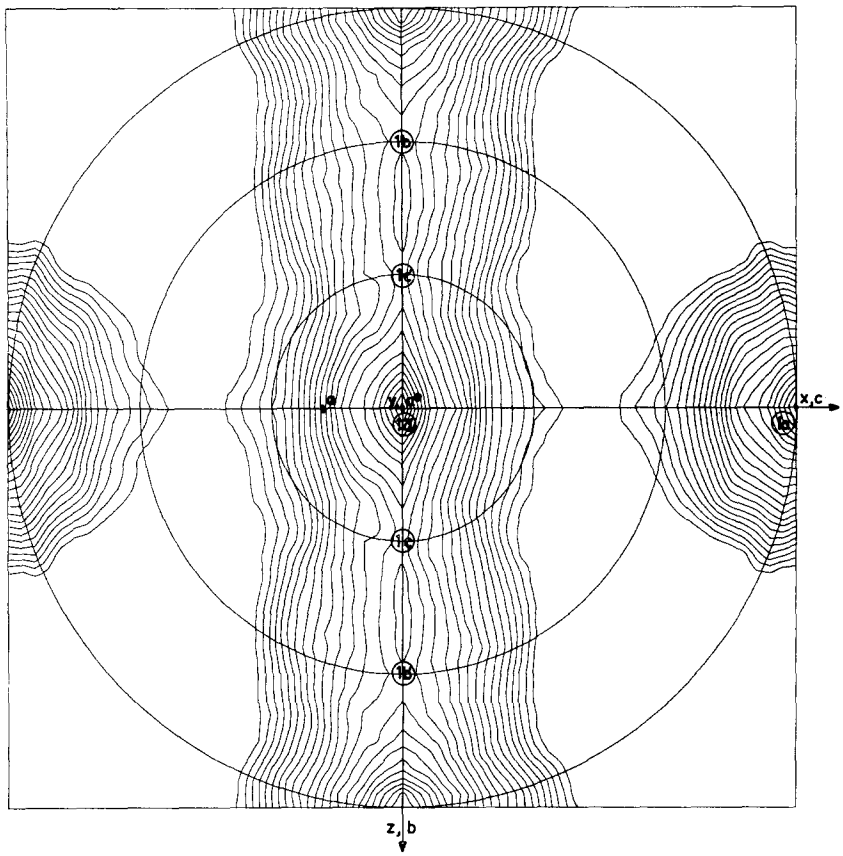

Fig. 5. Fast rotation function in reciprocal space. The strongest 9000 of the 13600 measured reflections in resolution range 5...3 Å were used. Only solution 1 is represented

being related by the crystallographic screw axis. This leads to the schematic model in Fig. 3.

Combination of the crystallographic screw axis with the local diads produces three local screw axes relating one tetramer to the other[3]. One of them, direction $\mathbf{b} \times (\mathbf{1a})$ is identical to $(\mathbf{1\tilde{a}})$. In the Patterson function this is a proper rotation axis relating one tetramer to another. The other two, $\mathbf{b} \times (\mathbf{1b})$ and $\mathbf{b} \times (\mathbf{1c})$ are improper rotation axes parallel to (**1a**), the rotation angle being twice the inclination angle of the local diads to the crystal screw axis, that is about 60° and 120° respectively. These axes are confirmed in the $\varkappa$-scan (Fig. 4) with the **c**-axis kept constant as rotation axis. They are also the strongest peaks in the stereograms for $\varkappa = 60°$ or 120°, respectively. Since they are improper rotation axes, relating 4 monomers to 4 different ones, the associated peak height is expected to be about half the value of the 180°-rotation, which relates all 8 monomers.

[3] Such axes have previously been called "packing symmetry" (Klug, 1971).

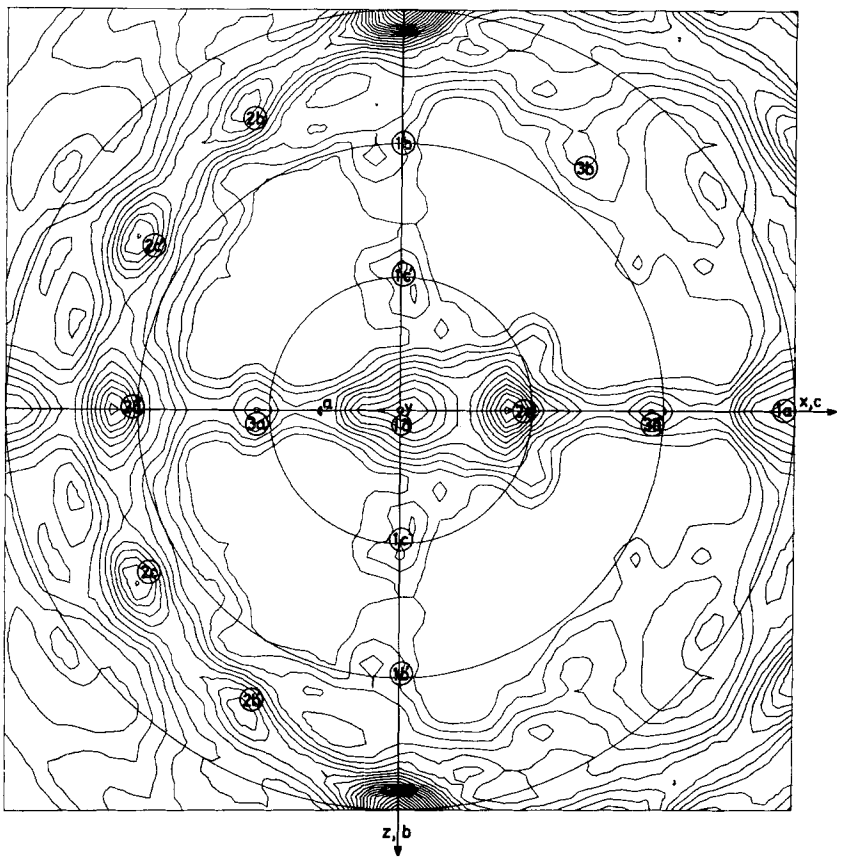

Fig. 6. Fast rotation function in reciprocal space; resolution limit 20...7 Å; all 4600 measured intensities were used. Solution 2 is the dominant feature; solution 1 and peaks (3) are comparatively poorly represented

Discrimination between rotation and screw axes is described in the next section (disc rotation).

The foregoing also holds for the peaks marked (2a), (2b), (2c), (2ã). The model in Fig. 3 remains valid except that the horizontal axis is no longer parallel to **a***.

The remaining peaks (3) turn out to be 4-fold axes at low resolution.

We have then to discriminate between the two solutions 1 and 2. This has been done by calculating different rotation functions as a function of both the resolution limits of the diffraction data and the radius of integration around the Patterson function origin.

All "fast rotation functions" calculated from data with resolution higher than 6 Å resembled Fig. 5, showing only solution 1. Peak (1a) is nearly as strong as the crystallographic axis, as is theoretically expected, since these local diads are parallel in both tetramers thus relating 8 subunits. The axes (**1b**) and (**1c**) are not resolved. From the peak heights it can be concluded that these axes do not have

Table 1

R_1	R_2	Π_1	Π_2	Π_1/Π_2	M mean value of rotation function	Π_1*	Π_2*	Π_1*/Π_2*
10 Å	15 Å	209000	135000	1.55	28	27300	11500	2.38
6 Å	20 Å	205000	178000	1.15	38	7400	5600	1.32
6 Å	35 Å	68000	75000	0.91	25	3100	4800	0.65
20 Å	35 Å	98	2200	0.045	− 3	410	4200	0.097
35 Å	50 Å	660	890	0.74	3	165	320	0.52

R_1, R_2 = inner, outer Patterson radius.
Π_x = Xa × Xb × Xc, the triple product of associated peak heights where X = 1 or 2.
Π_x* = (Xa − M) × (Xb − M) × (Xc − M), where M is the mean value of the rotation function under consideration.

identical inclination angles of 45°. In this case axis (**1b**) would be parallel to (**1c'**), and (**1c**) to (**1b'**), so that the peak height should nearly equal the peak due to the crystallographic axis. In fact it is only 70% as high as this indicating overlap of two neighbouring peaks of half the height of (1a). Furthermore the improper rotation axes parallel to the c-axis would then be 90°-axes (see Fig. 4).

If on the other hand low resolution data are used (below 6 Å), the rotation function changes completely: Solution 2 becomes the dominant feature, whereas the "high resolution peaks" are now only minor peaks (Fig. 6).

Further discrimination between solution 1 and 2 is provided by the radius dependence of the rotation function. This is a feature typical of the real space rotation programs: only vectors between R_1 and R_2 are used in the correlation function. As a simple analogon to the "locked rotation function" (Rossmann, 1972) the heights of the associated peaks of either 222 symmetry solution were multiplied; Table 1 summarizes the results. Clearly the relation between (solution 1): (solution 2) decreases with the radius limits.

Moreover the positions of the solution 2 peaks shift as the radius and resolution limits are varied, wheras the solution 1 peaks remain fixed in all rotation function calculations.

From all these observations we conclude that the molecular symmetry of the tetramer is given by solution 1, whereas solution 2 represents "solvent symmetry". Further evidence for this conclusion is given in section IV based on model calculations.

b) Disc-Rotation: Each local rotation symmetry produces a local Harker-plane of particularly high vector density, which contains the origin if and only if the symmetry is pure rotation without screw component (Colman *et al.*, 1975). The orientation of such local Harker planes can be found by the method of disc rotation, *i.e.* a special rotation function correlating a disc of unit density with the Patterson map, or in other words an integration of the Patterson density on a plane within the radius of the disc. This method of disc rotation discriminates between pure rotation and screw axes; it does not discriminate between rotations of different angle.

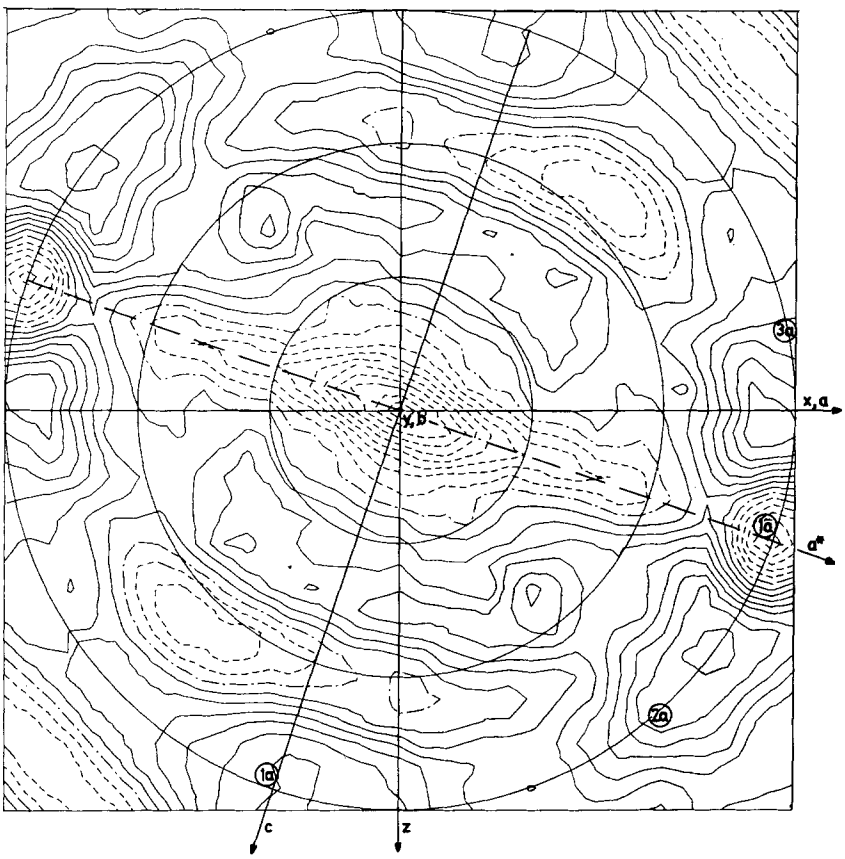

Fig. 7. Disc rotation function using the 3 Å-Patterson function and a disc of 20 Å radius. Contribution of Patterson origin removed by cutting out the centre of the disc within 3 Å radius. Stereogram for the direction of the disc normal, equivalent to the associated rotation axis direction (see text)

In practice we have taken a horizontal disc (polar coordinates of the normal: $\psi = 0$) and rotated it about an axial direction (ψ_a, φ_a), with rotation angle $\varkappa \equiv 180°$. After this rotation the polar coordinates of the disc normal are $\psi_n = 2\,\psi_a$, $\varphi_n = \varphi_a$. The Harker planes associated with the local axes in Fig. 2 are found in the range $0 \leq \psi_a \leq 45°$.

The result of the rotation of a disc of 20 Å radius in the 3 Å Patterson map is shown as the stereogram for (ψ_n, φ_n, $\varkappa = 180°$) in Fig. 7. The local (**b**) and (**c**) axes are not represented, presumably because they relate only 4 out of 8 monomers. There is clear discrimination between the local rotation axis (**1a**) and the local screw axis (**1ã**). There are negative values of the correlation function for the crystallographic screw axis **b** as well.

III. Positioning the Molecules in the Crystal Cell

a) Disc Translation: Translation of the disc in its original orientation parallel to the a-c-plane along the **b**-axis did not show the expected maximum at b/2, signalling

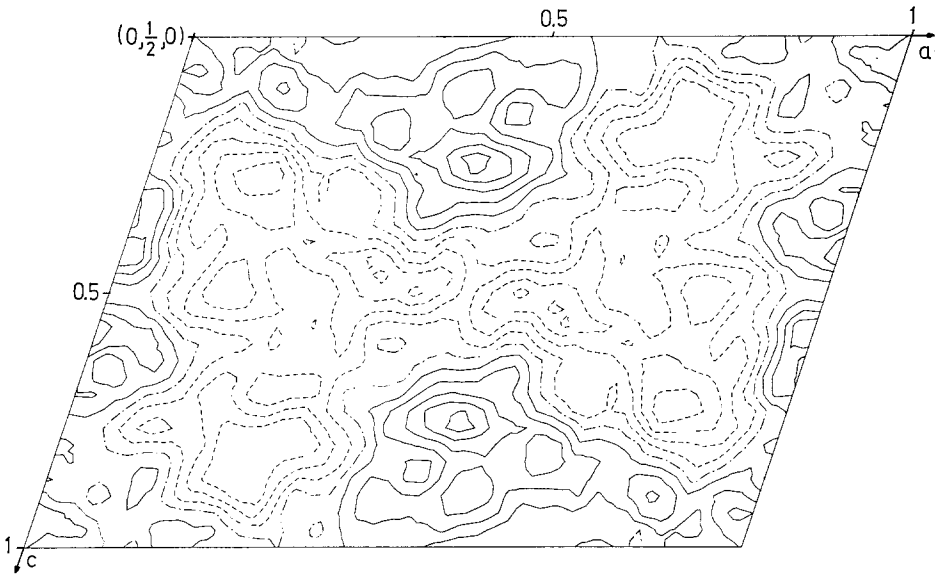

Fig. 8. Disc translation function: a disc of radius 20 Å is translated on the crystallographic Harker plane and the Patterson density integrated within the disc radius. Mean value dotted and dashed; solid contour lines indicate integrated density above mean value, dashed lines below mean value

the crystallographic Harker plane. The Harker vectors between the two tetramers in the unit cell have x and z components larger than the radius of the disc and hence were not detected. Translation of the disc within the Harker plane and correlation of disc and Patterson function density as function of disc position should provide a means of locating the centre of this set of Harker vectors. Such a technique was subsequently tested on the known structures of the Bence-Jones protein fragments *Rei* and *Au* with success limited in these cases by high space group symmetry (Colman *et al.*, 1975).

The result of the disc translation function, using a disc of 20 Å radius, is shown in Fig. 8. The highest peak is centred at (0.45/0.5/0.24) fractional coordinates; its height above mean value is 1.35 times the next highest peaks at (0/0.5/0.43) and (0.32/0.5/0.18).

b) Translation Function of Rossmann et al. (1964): Whenever two molecules (P, Q) in a crystal cell are related by a twofold screw axis, the cross vector sets (P→ Q and Q→ P) are also related by a screw axis through the origin parallel to the original one and with twice its translation component. Rossmann *et al.* (1964) designed their translation function in reciprocal space to find such cross vector sets in the Patterson map, and thus the cross vector between the molecules. The translation component of the screw (= distance of the Harker section from the origin) is found to be a "precise parameter" of this translation function, whereas the distances of the molecules from the screw axis are only imprecisely determined.

The cross vector sets of the phosphorylase tetramers are centred on the crystallographic Harker planes $y = b/2$, so the translation function is two-dimensional and was easily programmed in real space.

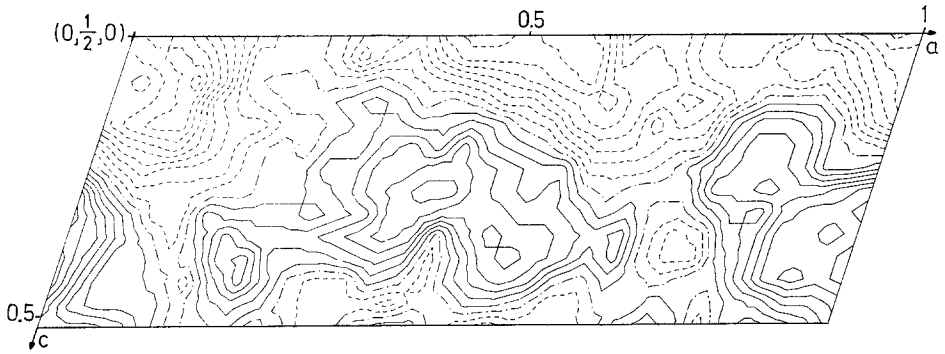

Fig. 9. Rossmann *et al.* (1964) translation function using the crystallographic screw axis. Section y ≡ b/2

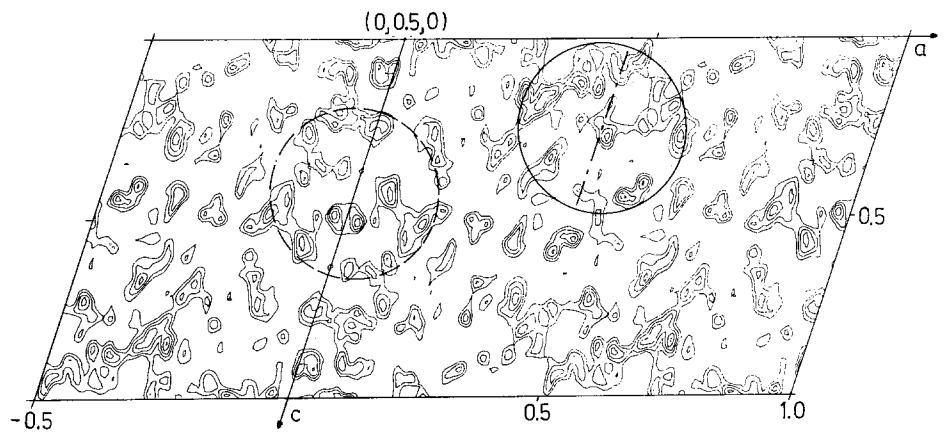

Fig. 10. Harker plane (y = b/2) of 3 Å-Patterson function calculated from all intensity data available. The solid circle encloses the maximum density of the disc translation function; the dashed circle indicates the additional solution in the translation function according to Rossmann *et al.* (1964)

The distance between the centres of the two tetramers in the unit cell can be determined either by use of the crystallographic screw axis or the local screw axis ($1\tilde{a}$). Use of the crystallographic screw axis implies determination of the imprecise parameters (x and z coordinates of the tetramer centre) since the screw component is in this case known. Such a search reduces to evaluation of the total density in a sphere of the Patterson function as a function of the position of the centre of the sphere in the Harker section. Clearly this function is analogous to the disc translation. This result (Fig. 9) is equivocal. Apparently the sphere contains too many noise vectors, which do not belong to the cross vector sets in question.

Use was then made of the local screw axis ($1\tilde{a}$), which is parallel to the **a*** axis. Now the distance from the crystallographic axis parallel to the local screw is a "precise parameter". The symmetry of this set of cross vectors is equivalent to a

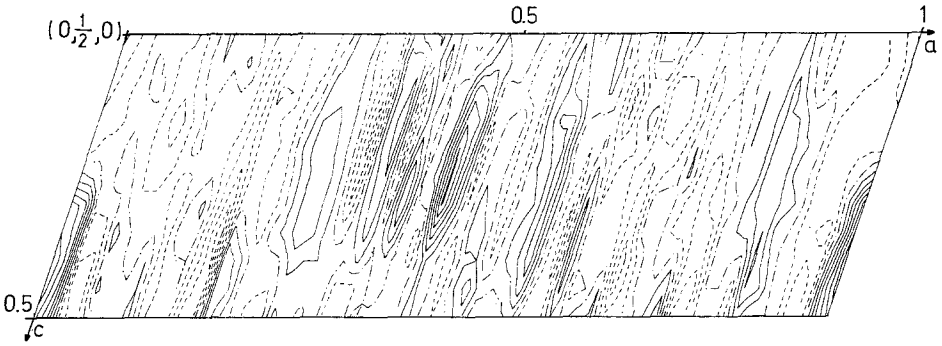

Fig. 11. Rossmann *et al.* (1964) translation function using the local screw axis (1ã). Section y≡ b/2

local mirror perpendicular to the local screw and centred on the crystallographic Harker plane. Such a mirror was readily found in the region around the maximum peak of the disc translation function when inspecting the Patterson map by eye (Fig. 10). This solution also results from the complete calculation (Fig. 11), though there is an equally strong maximum coinciding with the second peak at (0, 0.5, 0.43) in the disc translation. The meaning of this solution is yet unclear; from the model building (see next paragraph) this peak is unlikely to be the tetramer-tetramer cross vector.

IV. Model Calculations

The aim of these calculations at 7 Å resolution was to explain the meaning of the rotation function solution 2.

A dimer was represented by two spheres of 30 Å radius in close contact. This simple model seems to be not too far from truth given the Oxford model of the phosphorylase *b* dimer (Johnson *et al.*, 1974) which has overall dimensions of 116 Å × 63 Å × 63 Å.

Different 222 symmetric models, consistent with solution 1, were constructed, ranging from a structure in which the monomers were centred at the corners of a tetrahedron to one in which they were situated at the corners of a square. In these two extreme cases bad contacts between neighbouring molecules existed (in the **c** and **a*** directions respectively). An intermediate model (Fig. 12) in which the long axes of the two dimers sustended an angle of $\sim 60°$ with each other did not violate the unit cell space requirement in the a-c-plane. Such considerations are independent of the relative positions of the two tetramers in the unit cell.

Two tetramers of the shape described above fit most satisfactorily into the $P2_1$ unit cell when the tetramer center is that given by the disc translation function. The other translation function solution leads to severe overlap of the two tetramers.

Structure factors and intensities were calculated from this model density assuming constant electron density within the spheres, and subsequently used in a fast rotation function calculation.

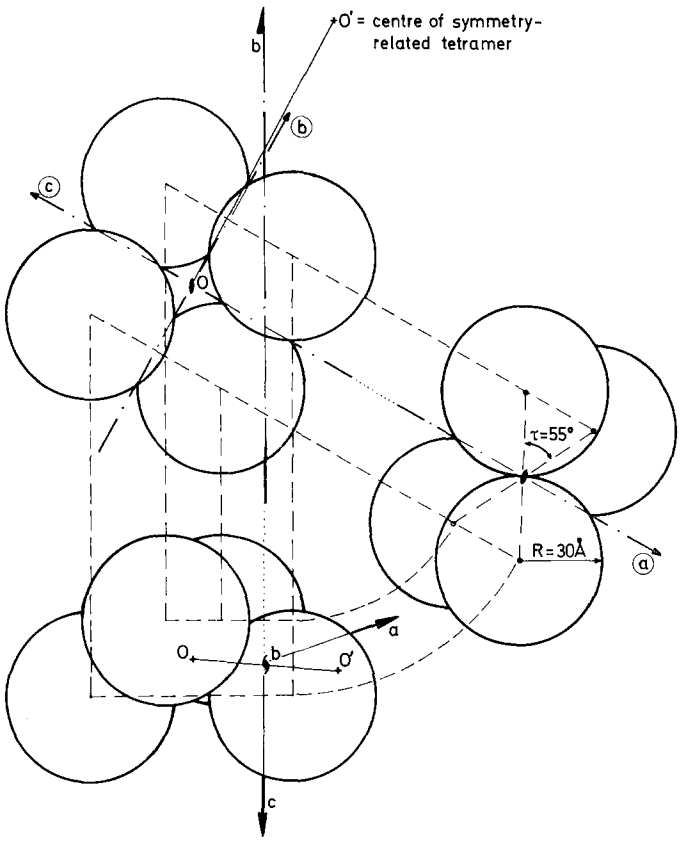

Fig. 12. Tetrameric model described in the text. Three projections down the crystallographic c and b axis and the molecular (c) axis, respectively, are drawn. The tetramer-tetramer cross vector is **00′**

The search radius around the Patterson origin in these model rotation functions at 7 Å resolution was always 35 Å (*i.e.* the maximum allowed under the present fast rotation function program restrictions).

The first rotation function with monomer radii of 30 Å (as described above) showed no evidence of solution 1 from which the model was built. This result, however, compares well with the very weak indication for solution 1 found in the low resolution phosphorylase data (Fig. 6). The intratetrameric cross vectors are in this case *quasi* spacefilling within the integration radius, so in an attempt to introduce more contrast into the model, the monomer radii were reduced to 25 Å; their centres were not altered. A comparable rotation function now showed some indication of solution 1, similar in fact to that seen in Fig. 6. Both of the above model calculations show strong indications of solution 2.

In the latter case (spheres of 25 Å radius) all peaks of this "solvent symmetry" are present and well resolved (Fig. 13) and only slightly shifted as compared to Fig. 6. The peak shifts could possibly be used to refine the relative position of the

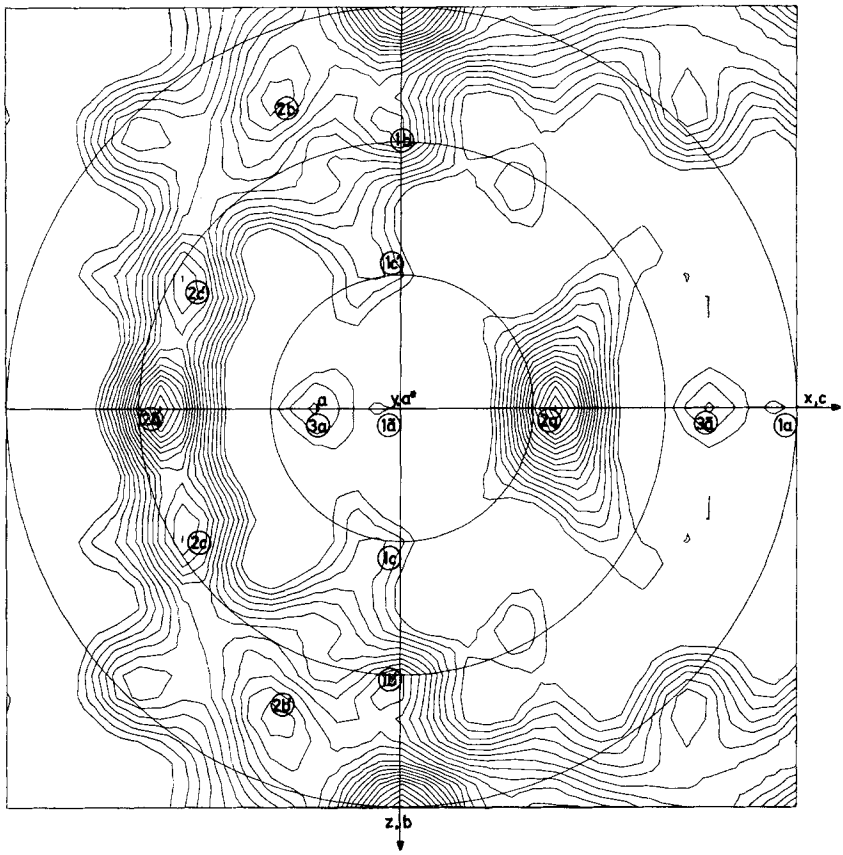

Fig. 13. Fast rotation function of the model built from spheres according to the molecular symmetry (solution 1) and placed in the cell according to the solution of the disc translation for resolution limit 20...7 Å; Patterson radius 35 Å. The strongest 9000 of the 11600 calculated triclinic structure factors were used. Apart from (3b) all peaks from Fig. 6 show up

spheres within the tetrameric model; they may also be due to the non spherical shape of the phosphorylase monomers.

Conclusions

Tetrameric phosphorylase *a* exhibits molecular 222 symmetry. One of the local diads is perpendicular to the crystallographic screw axis **b** and parallel to the **c**-axis of the unit cell. The other two local diads lie in the **b**,**a***-plane and are inclined about $\pm$ 30° and $\pm$ 60° respectively to the crystallographic screw axis. The vector products of the local diads with the crystallographic screw axis yield 3 local screw axes, one of which is a diad parallel to the **a***-axis. The other two are improper rotation axes with rotation angles 60° and 120°, which in either case is twice the inclination of the associated local diad to the **b**-axis. These local screw axes indicate "packing symmetry".

In addition the low resolution data show a set of symmetry axes which have been interpreted as "solvent symmetry", *i.e.* correlation of cross vectors between neighbouring monomers which belong to different tetramers. In other words, these axes put protein onto protein and solvent onto solvent, regardless of the inner structure of the protein. This interpretation has been confirmed by the rotation function calculation using a model consisting of homogeneous spheres.

The construction of the model required the knowledge of the position of the tetramers relative to the crystallographic screw axis or equivalently relative to each other. The distance of the centre of the tetramers from the crystallographic diad is approx. 1/4 the cell width in the direction of the **a*** axis.

The model tetramer was built from spherical monomers arranged according to the molecular 222 symmetry; the relative orientation of the dimers within the tetramer was chosen to provide optimal space filling in the **a**-**c**-plane. When the symmetry related tetrameric models were placed in the cell using the result of the disc translation as tetramer-tetramer cross vector, there is minimum overlap between the tetramers.

Future plans include the detection of the known structure of phosphorylase *b* (Johnson *et al.*, 1974) in the phosphorylase *a* cell which would provide independant confirmation of the results described before. There might then be a possibility to extend the phases using the known molecular symmetry (Colman, 1974; Bricogne, 1974).

Acknowledgements. We wish to thank Dr. R. Huber and our colleagues, especially H. Fehlhammer, for helpful discussions. The financial assistance of the DFG and SFB 51 is gratefully acknowledged.

References

Bricogne, G.: Geometric sources of redundancy in intensity data and their use for phase determination. Acta Cryst. **A30**, 395–405 (1974)

Campbell, I. D., Dwek, R. A., Price, N. C., Radda, G. K.: Studies on the interaction of ligands with phosphorylase *b* using a spin-label probe. Europ. J. Biochem. **30**, 339–347 (1972)

Colman, P. M.: Noncrystallographic symmetry and the sampling theorem. Z. Krist. **140**, 344–349 (1974)

Colman, P. M., Fehlhammer, H., Bartels, K.: Patterson search methods in protein structure determination: β-trypsin and immunoglobulin fragments. In: Crystallographic computing (ed. F. R. Ahmed). Copenhagen: Munksgaard 1975

Crowther, R. A.: The fast rotation function. In: The molecular replacement method (ed. M. G. Rossmann), pp. 173–178. New York-London-Paris: Gordon & Breach 1972

Dwek, R. A., Griffiths, J. R., Radda, G. K., Strauss, U.: A spin label probe for the conformational change on conversion of phosphorylase *b* to phyosphorylase *a*. FEBS Letters **28**, 161–164 (1972)

Eagles, P. A. M., Johnson, L. N., Joynson, M. A., McMurray, C. H., Gutfreund, H.: Subunit structure of aldolase: Chemical and crystallographic evidence. J. molec. Biol. **45**, 533–544 (1969)

Epp, O., Steigemann, W., Formanek, H., Huber, R.: Crystallographic evidence for the tetrameric subunit structure of L-asparaginase from *Escherichia coli*. Europ. J. Biochem. **20**, 432–437 (1971)

Fasold, H., Ortanderl, F., Huber, R., Bartels, K., Schwager, P.: Crystallization and crystallographic data of rabbit muscle phosphorylase *a* and *b*. FEBS Letters **21**, 229–232 (1972)

Fehlhammer, H.: Dissertation, Technische Universität München (1975)

Griffiths, J. R., Price, N. C., Radda, G. K.: Conformational changes in phosphorylase *a*, studied by a spin label probe. Biochim. biophys. Acta (Amst.) **358**, 275–280 (1974)

Hoppe, W.: Die Faltmolekülmethode und ihre Anwendung in der röntgenographischen Konstitutionsanalyse von Biflorin ($C_{20}H_{20}O_4$). Elektrochem. **61**, 1076—1083 (1957)

Huber, R.: Programmed "Faltmolekül" method. In: Crystallographic computing (ed. F. R. Ahmed), pp. 96—102. Copenhagen: Munksgaard 1970

Johnson, L. N., Madsen, N. B., Mosley, J., Wilson, K. S.: The crystal structure of phosphorylase *b* at 6 Å resolution. J. molec. Biol. **90**, 703—717 (1974)

Kiselev, N. A., Lerner, F. Ya., Livanova, N. B.: Electron microscopy of muscle phosphorylase *b*. J. molec. Biol. **62**, 537—549 (1971)

Kiselev, N. A., Lerner, F. Ya., Livanova, N. B.: Electron microscopy of muscle phosphorylase *a*. J. molec. Biol. **86**, 587—599 (1974)

Klug, A.: Interpretation of the rotation function map of satellite tobacco necrosis virus: Octahedral packing of icosahedral particles. Cold Spr. Harb. Symp. quant. Biol. **36**, 483—487 (1971)

Madsen, N. B., Honickel, K. O., James, M. N. G.: Studies on glycogen phosphorylase in solution and in the crystalline state. 2nd Int. Symp. on Metabolic Interconversion of Enzymes (eds. O. Wieland, E. Helmreich, H. Holzer), pp. 55—72. Berlin-Heidelberg-New York: Springer 1972

Mathews, F. S.: X-ray crystallographic study of glycogen phosphorylase. Fed. Proc. **26**, 831 (1967)

Rossmann, M. G., Blow, D. M.: The detection of sub-units within the crystallographic asymmetric unit. Acta Cryst. **15**, 24—31 (1962)

Rossmann, M. G., Blow, D. M., Harding, M. M., Coller, E.: The relative positions of independent molecules within the same asymmetric unit. Acta Cryst. **17**, 338—342 (1964)

Rossmann, M. G.: The locked rotation function. Appendix in Rossmann, M. G., Ford, G. C., Watson, H. C., Banaszak, L. J.; J. molec. Biol. **64**, 237—249 (1972)

Schwager, P., Bartels, K., Huber, R.: A simple empirical absorption-correction method for X-ray intensity data films. Acta Cryst. **A29**, 291—295 (1973)

Schwager, P., Bartels, K., Jones, A.: Refinement of setting angles in screenless film methods. J. appl. Cryst. 8, 275—280 (1975)

Schwager, P., Bartels, K.: The Munich Program System for X-Ray Intensity Data Film Evaluation by Off-Line-Computer (Tentative Title). Proceedings of the Groningen symposium on the rotation method (Feb. 75) (eds. U. W. Arndt, A. J. Wonacott). Amsterdam: Elsevier North Holland Publ. Corp. 1975

Steigemann, W.: Dissertation, Technische Universität München (1974)

Tollin, P., Rossmann, M. G.: Errata in Rossmann and Blow (1962). Appendix in Acta Cryst. **21**, 876 (1966)

Received August 15, 1975/Accepted December 18, 1975